*Materials*

# Ageing behavior of an Al-Zn-Mg-Cu alloy pre-stretched thick plate

*Zhihui Li, Baiqing Xiong, Yongan Zhang, Baohong Zhu, Feng Wang, and Hongwei Liu*

State Key Laboratory for Fabrication and Processing of Non-ferrous Metals, General Research Institute for Non-ferrous Metals, Beijing 100088, China
(Received 2006-11-27)

**Abstract:** The ageing behavior of a pre-stretched thick plate of Al-Zn-Mg-Cu alloy was systemically studied including one-step ageing, two-step ageing, and retrogression and reageing treatment (RRA). One-step ageing of the alloy resulted in peak ultimate tensile strengths of 595 and 575 MPa after 22 and 6 h at 120 and 135°C, respectively. The strengthening phase in peak aged (T6 temper) alloy contained GP zones and the η′ phase predominantly. After two-step ageing, the electrical conductivity was increased markedly, but the pre-stretched thick plate sacrificed a great loss of strength. RRA treatment provided a method for maintaining the strength close to that obtained by T6 temper and for obtaining the high electrical conductivity close to that obtained by T7 temper; the ultimate tensile strength and electrical conductivity were 583 MPa and 21.0 MS/m, respectively. TEM analysis of T7 and RRA specimens revealed two types of precipitates that contributed to age strengthening *i.e.* the η′ and η phases.

**Key words:** Al-Zn-Mg-Cu alloy; pre-stretched thick plate; ageing; tensile properties; precipitation

## 1. Introduction

Al-Zn-Mg-Cu alloys are widely used for structural applications in aerospace because of their specific mechanical properties. With the development of high speed milling machines and the improved properties of thick plates, large structures machined from a thick plate can now replace forged components or built-up structures, which significantly reduce the cost by minimizing the amount of components and joints [1-5]. More recently, thick plates of Al-Zn-Mg-Cu series alloys were used extensively in the aircraft and aerospace industry [6-9].

Al-Zn-Mg-Cu series alloys are typical ageing precipitate strengthening alloys; the ageing treatment is a key process to achieve the required microstructures and properties. T6 temper can obtain the peak hardness and tensile strength, with high stress corrosion cracking (SCC) susceptivity [10]. The T7 temper increases the stress corrosion resistance of Al-Zn-Mg-Cu series alloys by modifying the microstructures, sacrificing about 10%-15% of the tensile strength properties with respect to peak-aged (T6 temper) alloys [11-12]. Retrogression and reageing (RRA) treatment was devised by Cina [13] and it was claimed to improve the SCC resistance of Al-Zn-Mg-Cu series alloys while maintaining their strength at the level of the peak-aged tem-

per. In general, RRA was suitable for the treatment of articles having thin section dimension because of the retrogression treatment lasting just for a few seconds to a few minutes at a relative high temperature of 200-260°C [14-16].

The purpose of the present article is to investigate in detail the ageing behavior of the pre-stretched thick plates of Al-Zn-Mg-Cu and to understand the ageing strengthening mechanism in different ageing conditions. In RRA treatment, the relative low retrogression temperature (180°C) was selected in this study to allow moderately thicker section components to be treated for a relative long time.

## 2. Experimental

The chemical composition of the alloy investigated in the present study was Al-6.23Zn-2.88Mg-1.58Cu-0.16Cr-0.31Mn-0.15Fe-0.048Si-0.025Ti (wt%). The slabs were prepared by the traditional ingot metallurgy process. After casting, the slabs were homogenized, scalped, hot-rolled to plates of 40 mm in thickness, solid solution treated at 470°C, water quenched (a roller-type spray quenching equipment was used) to room temperature, and pre-stretched (residual stress relieving). The bulk samples used in this research were obtained from a monolithic thick plate, and heat treated

by the one-step ageing, two-step ageing, and the retrogress and reageing (RRA) tempers. For the one-step ageing, the alloy was treated at 120 and 135°C for 0-72 h. The two-step ageing consisted of an initial ageing for 7 h at 115°C, followed by the second ageing at 165°C for 0-36 h. For the RRA temper, the alloy was subjected to a three-step ageing involving pre-ageing for 10 h at 120°C followed by retrogressing for 1.5 h at 180°C, and then reageing at the peak aged condition.

The tensile properties of the thick plate were evaluated with a nominal tension rate of 1 mm/min at room temperature in long transverse (LT) direction at 1/4 location of the plate thickness, using 25 mm gauge length specimens. Each datum is the average of three samples. Electrical conductivity measurement on the samples was carried out using a direct reading type conductivity meter. TEM specimens were prepared by cutting thin slices from the aged samples, which were then mechanically thinned down to ~50 μm and then electropolished using a twin-jet polisher with a 25vol% nitric acid solution in methanol at (−30)-(−20)°C with an applied voltage of 15-20 V. The microstructural characterization was carried out using a JEM 2000FX transmission electron microscope at 160 kV.

## 3. Results and discussion

### 3.1. One-step ageing treatment

The ageing curves for one-step ageing, as shown in Fig. 1, illustrate the ageing response of the alloy at 120 and 135°C, respectively. The peak ultimate tensile strength (UTS) values were 595 and 575 MPa at ageing temperatures of 120 and 135°C, respectively. The ageing time to achieve these peak UTS values were 22 and 6 h, respectively. These results indicated that the rate of strength increases markedly with increasing ageing temperature while the peak strength decreases. During the overageing stage, there are some quite significant ageing kinetics differences between these; more rapid kinetics was observed at 135°C than at 120°C. Furthermore, Fig. 1(c) shows the electrical conductivity as a function of the one-step ageing time for the alloy. It can be seen that electrical conductivity increases with increasing ageing time and ageing temperature. Following the research results of other researchers [17-19], electrical conductivity serves as an indicator of corrosion resistance, *i.e.*, the higher electrical conductivity means the material has a higher SCC performance.

The microstructure of the alloy after ageing for 22 h at 120°C (T6 temper) is shown in Fig. 2. It can be seen that the precipitates in the matrix are very fine and are distributed homogeneously, with their size ranging

from 3 to 6 nm; the grain boundary precipitates are semi-continuous and the precipitation free zone (PFZ) with about 10 nm width is presented. The diffraction spots from the aluminum matrix have been indexed; the weak spots from the GP zones and the η′ phase can be identified, indicating that the strengthening mechanism of the peak-aged alloy is GP zones and η′ phase strengthening in combination.
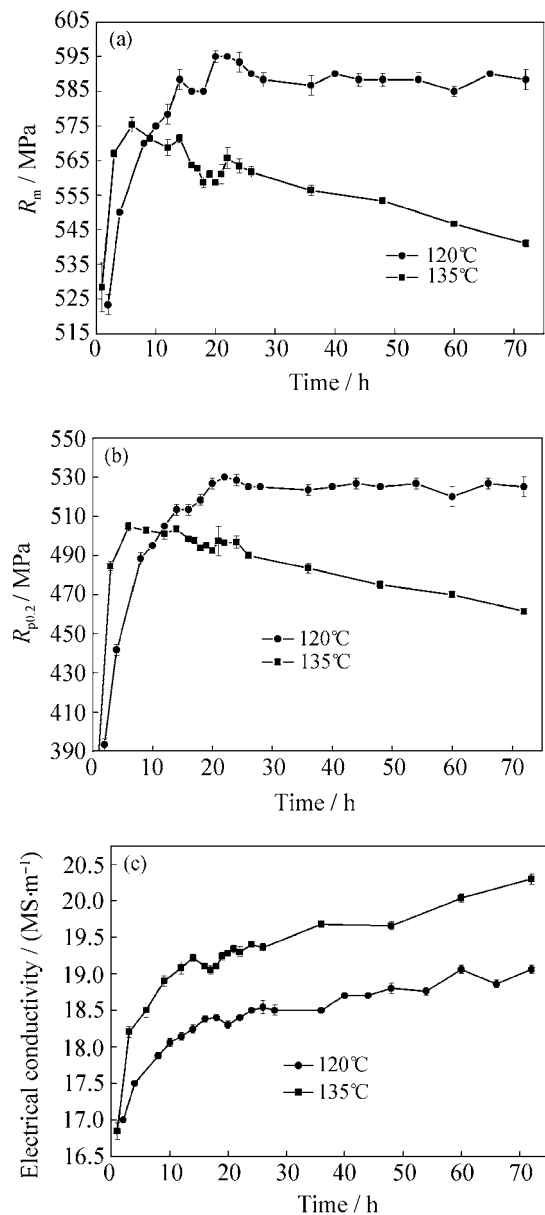


Fig. 1.  Ageing curves of one-step ageing at 120 and 135°C: (a) ultimate tensile strength; (b) 0.2% proof stress strength; (c) electrical conductivity.

### 3.2. Two-step ageing treatment

The two-step ageing involved pre-ageing for 7 h at 115°C, followed by final ageing at 165°C. The variation of the tensile strength and the electrical conductivity during the final ageing is plotted in Fig. 3. It can be seen that a peak tensile strength is achieved after 1-2 h at 165°C in the two-step ageing treatment; after the peak strength point, the tensile strength of the alloy de-

248

*J. Univ. Sci. Technol. Beijing, Vol.14, No.3, Jun 2007*

creases obviously while prolonging the final ageing time. On the other hand, the electrical conductivity of the alloy increases with the increase of final ageing time. By comparing with Fig. 1(c), it is found that the electrical conductivity after two-step ageing treatment increases remarkably; the electrical conductivity is

about 21 MS/m after ageing for 6-8 h, which is higher than that by the T6 temper (about 18.3 MS/m). It suggests that the SCC resistance of the alloy obtained by the two-step ageing temper is higher than that obtained by the peak-aged (T6 temper).
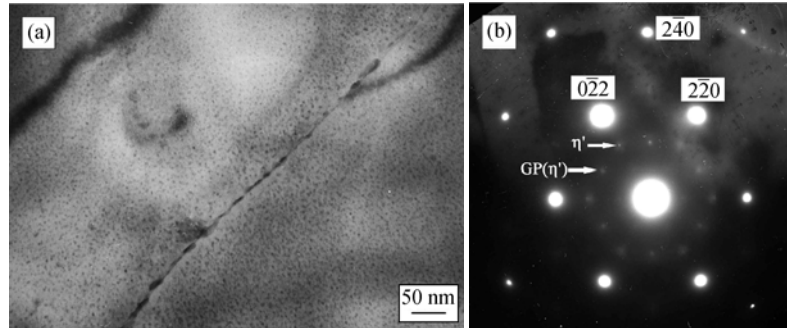


**Fig. 2.  TEM images of the alloy aged for 22 h at 120°C (T6 temper): (a) bright field image; (b) selected area diffraction (SAD) pattern taken along the [111]$_{Al}$ direction.**
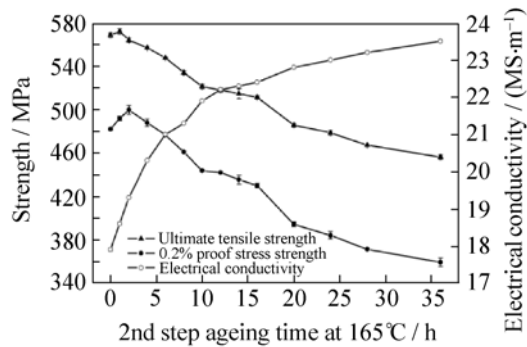


**Fig. 3.  Ageing curves of the two-step aged at 115°C for 7 h plus 165°C for various periods of time.**

Fig. 4 shows TEM images of the alloy after ageing for 7 h at 115°C plus 16 h at 165°C. It can be seen that the precipitates in the matrix increase remarkably, with their size ranging from 10 to 30 nm; the precipitation density is very low. It is not surprising that the alloy possesses low tensile strength under this ageing temper. Furthermore, the grain boundary precipitates, recognized as the η phase [20], grow up to be coarser and are more sparsely distributed, and the PFZ of 30-40 nm in width can also be observed. SAD patterns taken along the [100]$_{Al}$ and [112]$_{Al}$ directions are shown in Fig. 4(b) and Fig. 4(c), respectively, indicating the existence of the η′ phase and the η phase. The spots from the η′ phase and the η phase in the SAD patterns mentioned above have been marked by arrows and legends in the figures for better clarity. Based on the experimental results mentioned above, it can be considered that the strengthening mechanism for the two-step aged alloy is the η′ phase and the η phase strengthening in combination.

### 3.3. Retrogression and reageing treatment

Table 1 presents the tensile properties and the electrical conductivity of the alloy by RRA temper (T6 and

T7 tempers are listed for comparison). It can be noted that the differences between the tensile properties obtained in peak aged and RRA tempers are minimal. On the other hand, the electrical conductivity in the RRA temper is remarkably increased, which is higher than that in the peak aged alloy. It is suggested that the SCC resistance of the RRA treated alloy is improved obviously.

Fig. 5(a) shows a TEM micrograph of the alloy after RRA treatment. It can be found that the precipitates in the matrix are very similar to the T6 temper, which are very fine with their size ranging from 5 to 10 nm, and are distributed homogeneously. Therefore, it is not surprising that the tensile strength of the alloy in the RRA temper is very close to that obtained by the T6 temper. The grain boundary characteristics are similar to that obtained by the T7 temper (Fig. 4(a)); the precipitates are coarse and are discontinuously distributed. Following the viewpoints of the other researchers [21], the coarser and more discrete grain boundary precipitates have been suggested to improve the SCC resistance. Thus, it may be suggested that the RRA treatment is favorable for the SCC resistance of the alloy. Furthermore, apparent PFZ with 40-50 nm width along the grain boundary was observed.

Fig. 5(b) and Fig. 5(c) show SAD patterns taken along the [110]$_{Al}$ and [112]$_{Al}$ projection. The SAD pattern analysis indicates that extra spots are mainly from the η′ phase and the η phase, confirming that the primary microstructure at RRA temper contains the η′ phase and the η phase predominantly. Thus, the strengthening mechanism for the RRA treated alloy is the η′ phase and the η phase strengthening in combination.
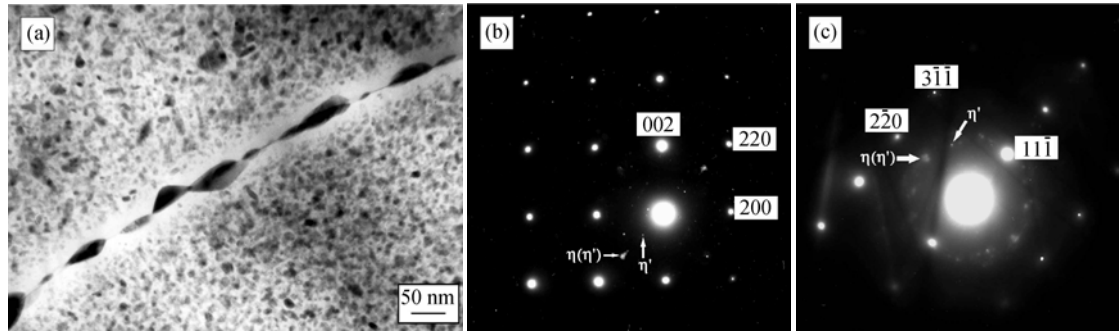
**Fig. 4.** TEM images of the alloy aged for 7 h at 115°C plus 16 h at 165°C: (a) bright field image; (b) SAD pattern taken along the [100]$_{Al}$ direction; (c) SAD pattern taken along the [112]$_{Al}$ direction.

**Table 1.** Tensile properties and electrical conductivity of RRA, T6, and T7 treated alloy pre-stretched thick plates (LT-long transverse)

| | Temper | | $R_m$ / MPa | $R_{p0.2}$ / MPa | $A$ / % | $\gamma$ / (MS·m$^{-1}$) |
|---|---|---|---|---|---|---|
| RRA | 120°C×10 h | 180°C×1.5 h+120°C×22 h | 583 | 525 | 10.0 | 21.0 |
| | T6 | 120°C×22 h | 595 | 534 | 11.5 | 18.3 |
| | T7 | 115°C×7 h+165°C×16 h | 512 | 430 | 10.6 | 22.4 |

Note: $R_m$ represents the ultimate tensile strength; $R_{p0.2}$ represents the 0.2% proof stress strength; $A$ represents the elongation; $\gamma$ represents the electrical conductivity.
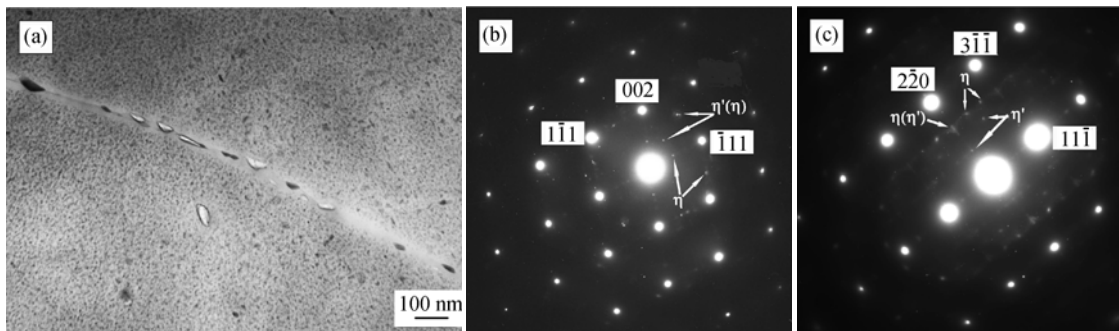


**Fig. 5.** TEM images of the alloy aged for RRA temper: (a) bright field image; (b) SAD pattern taken along the [110]$_{Al}$ direction; (c) SAD pattern taken along the [112]$_{Al}$ direction.

## 4. Conclusions

(1) One-step ageing of the alloy results in a peak UTS value of 595 MPa after 22 h at 120°C. After two-step ageing, the electrical conductivity increases markedly, but sacrifices a great loss of strength. RRA treatments provide a method for maintaining the strength close to that obtained by the T6 temper and for obtaining high electrical conductivity close to that obtained by the T7 temper; the UTS and electrical conductivity are 583 MPa and 21.0 MS/m, respectively.

(2) In the T6 temper, the alloy is strengthened by GP zones and the η′ phase strengthening in combination. The strengthening mechanism for both the two-step and the RRA treated alloy is the η′ phase and the η phase strengthening in combination.

(3) The grain boundary precipitates in the peak-aged

(T6 temper) alloy are fine and semi-continuously distributed. On the contrary, the grain boundary precipitates in both T7 and RRA treated alloys are coarse and discretely distributed.

## References

[1] A. Heinz, A. Haszler, C. Keidel, *et al.*, Recent development in aluminium alloys for aerospace applications, *Mater. Sci. Eng.*, A280(2000), p.102.

[2] C. Liu, Y. Bi, and R. Benedictus, Modelling Al₃Zr precipitation in an AA7050 alloy, [in] *Proc. 9th Int. Conf. Aluminium Alloys*, Australia, 2004, p.907.

[3] A.S. Warren, Developments and challenges for aluminum – A boeing perspective, [in] *Proc. 9th Int. Conf. Aluminium Alloys*, Australia, 2004, p.24.

[4] I.N. Fridlyander, A.V. Dobromyslov, E.A. Tkachenko, et al., Advanced high-strength aluminum-base materials, *Met. Sci. Heat Treat,* 47(2005), p.269.

[5] M.P. Miller, E.J. Harley, T.J. Turner, *et al.*, Mechanical

250

*J. Univ. Sci. Technol. Beijing, Vol.14, No.3, Jun 2007*

behavior of thin sheets machined from AA7050-T7451 plate, *Mater. Sci. Forum*, 331-337(2000), p.1243.

[6] B.H. Zhu, Y.A. Zhang, B.Q. Xiong, *et al*., Effect of artificial aging temper on the microstructure and properties of 7B04 pre-stretched thick plate, *Mater. Sci. Forum*, 519-521(2006), p.901.

[7] A.K. Mukhopadhyay, G.M. Reddy, K.S. Prasad, *et al*., Microstructure property relationships in a high strength Al-Zn-Mg-Cu-Zr alloy, [in] *Proc. 9th Int. Conf. Aluminium Alloys*, Australia, 2004, p.883.

[8] H.Z. Zhou, Aluminum alloy pre-stretched thick plates, *Alum. Fabr.* (in Chinese), 22(1999), No.3, p.16.

[9] Z.H. Li, B.Q. Xiong, Y.A. Zhang, *et al*., Effect of the one-step ageing on microstructure and properties of 7B04 pre-stretched thick plate, *Chin. J. Nonferrous Met.* (in Chinese), 15(2005), No.11, p.1670.

[10] I.J. Polmear, Aluminium alloys—a century of age hardening, [in] *Proc. 9th Int. Conf. Aluminium Alloys*, Australia, 2004, p.1.

[11] J.C. Werenskiold, A. Deschamps, and Y. Brechet, Characterization and modeling of precipitation kinetics in an Al-Zn-Mg alloy, *Mater. Sci. Eng.*, A293(2000), p.267.

[12] J.K. Park and A.J. Ardell, Microstructure of the commercial 7075 Al alloy in the T651 and T7 tempers, *Metall. Trans.*, 14A(1983), p.1957.

[13] B. Cina and B. Ranish, *New Technology for Reduceing Susceptibility to Stress Corrosion of High Strength Aluminium Alloys*, U.S. Patent, 3856584, 1974.

[14] A.F. Oliveira, Jr. de Barros, K.R. Cardoso, *et al*., The effect of RRA and SCC resistance on AA7050 and AA 7150 aluminium alloys, *Mater. Sci. Eng.*, A379(2004), p.321.

[15] N.C. Danh, K. Rajan, and W. Wallace, A TEM study of microstructural changes during retrogression and reaging in 7075 aluminum, *Metall. Trans.*, 14A(1983), p.1843.

[16] M.H. Brown, *Three-step Aging to Obtain High Strength and Corrosion Resistance in Al-Zn-Mg-Cu alloys*, U.S. Patent, 4477292, 1984.

[17] D.K. Denzer, D.J. Chakrabarti, J. Liu, *et al*., *Method for Increasing the Strength and/or Corrosion Resistance of 7000 Series Al Aerospace Alloy Products*, U.S. Patent, 20030051784, 2003.

[18] C.P. Ferrer, M.G. Koul, B.J. Connolly, *et al*., Improvements in strength and stress corrosion cracking properties in aluminum alloy 7075 *via* low-temperature retrogression and re-ageing heat treatments, *Corros. Sci.*, 59(2003), No.6, p.520.

[19] T.C. Tsai and T.H. Chuang, Relationship between electrical conductivity and stress corrosion cracking susceptibility of Al 7075 and Al 7475 alloys, *Corros. Sci.*, 52(1996), No.6, p.414.

[20] A.K. Mukhopadhyay, K.S. Prasad, V.K. Varma, *et al*., Influence of small additions of Sc and Ag on the microstructure and properties of Al alloy 7017, [in] *Proc. 9th Int. Conf. Aluminium Alloys*, Australia, 2004, p.793.

[21] M. Puiggali, A. Zielinski, J.M. Olive, *et al*., Effect of microstructure on stress corrosion cracking of an Al-Zn-Mg-Cu alloy, *Corros. Sci.*, 40(1998), No.4/5, p.805.